Cold Regions Science and Technology 102 (2014) 8–20

Contents lists available at ScienceDirect

Cold Regions Science and Technology

journal homepage: www.elsevier.com/locate/coldregions

Interannual and seasonal variability in evapotranspiration and energy partitioning over the alpine riparian shrub *Myricaria squamosa* Desv. on Qinghai–Tibet Plateau

Si-Yi Zhang [a,b], Xiao-Yan Li [a,b,*], Yu-Jun Ma [a,b], Guo-Qin Zhao [b], Liu Li [b], Ji Chen [c], Zhi-Yun Jiang [b], Yong-Mei Huang [b]

[a] State Key Laboratory of Earth Surface Processes and Resource Ecology, Beijing Normal University, Beijing 100875 China
[b] College of Resources Science and Technology, Beijing Normal University, Beijing 100875 China
[c] Key Lab of Aerosol Science & Technology, SKLLQG, Institute of Earth Environment, Chinese Academy of Sciences, Xi'an 710075 China

ARTICLE INFO

Article history:
Received 9 August 2013
Accepted 14 February 2014
Available online 19 February 2014

Keywords:
Bowen ratio
Energy balance
Latent heat flux
Sensible heat flux
Freeze–thaw cycle
Qinghai Lake watershed

ABSTRACT

The Qinghai–Tibet Plateau is a sensitive area of global climate changes, and riparian ecosystems are thought as "hotspots" for climate change adaptation, but little work has been conducted regarding the alpine riparian ecosystems on the Qinghai–Tibet Plateau. We measured evapotranspiration (*ET*) and surface energy fluxes over the riparian shrub *Myricaria squamosa* Desv., which is widely distributed on the Qinghai–Tibet Plateau but has not been studied until now. The results indicated that annual *ET* was 390 mm and 503 mm for the period of 2010 to 2011 and 2011 to 2012, respectively, which was higher than the amount of precipitation during the same period. Cumulative *ET* was lower than the cumulative reference evapotranspiration during the entire experimental period, whereas *ET* in August was higher than reference evapotranspiration. *ET* in the growing season occupied over 80% of annual *ET* with a maximum daily *ET* of 7.2 mm d^{-1}, and the *ET* in the non-growing season was quite low because of the frozen soil. In general, temperature and net radiation were the key variables controlling daily *ET* rates for *M. squamosa*. Annual sensible heat flux (*H*) consumed 60% of net radiation (R_n) and latent heat flux (*LE*) 40% during the three years of the study. *LE* occupied the main part of R_n from July to September. *H* was the highest in May and June, then sunk in the mid-growing season, and rebounded the other peak at late September and early October. Daily ground heat flux was positive from April to mid-September, and it was an important heat source of land surface in the winter and spring. This study highlighted that as an alpine riparian ecosystem in a semiarid region, *ET* and surface energy partitioning of the *M. squamosa* community are strongly affected by the freeze–thaw cycle, groundwater fluctuation, precipitation pulses and soil water content. We speculate that climate warming has a significant impact on *ET* process and surface energy partitioning of the *M. squamosa* community by influencing the freeze–thaw cycle and soil water content.

1. Introduction

The Qinghai–Tibet Plateau is approximately 2.57 million km^2 in area and, with an average elevation of greater than 4000 m above sea level, is the highest plateau in the world (Zhang et al., 2002). Energy and water cycles in terrestrial ecosystems play a key role in climate change (Betts et al., 1999; Pielke et al., 1998), and in particular, those over the Qinghai–Tibet Plateau are suggested to play key roles in the progress of Asian monsoons (Tanaka et al., 2001; Zhang et al., 2003). To better understand the mechanism and dynamics of the energy cycle over the Asian Monsoon region, it is important to estimate the energy partitioning over the Qinghai–Tibet Plateau surface (Tanaka et al., 2001). As a sensitive area of global climate changes (Klein et al., 2004), recent studies have found that the Qinghai–Tibet Plateau has displayed a significant warming trend over recent decades (Kang et al., 2010; Wu et al., 2013; You et al., 2010). These climate changes will affect the energy exchange between the land surface and the atmosphere (Gu et al., 2005). Therefore, assessing the energy partitioning and evapotranspiration (*ET*) in the alpine ecosystems on the Qinghai–Tibet Plateau may provide insights into not only the energy and water cycle in the alpine ecosystems but also the local and even regional climate changes. The heat and water fluxes have been studied on the Qinghai–Tibet Plateau under the auspices of the GAME/Tibet, CAMP/Tibet and ChinaFLUX, as well as other research projects (Gu et al., 2005; Hu et al., 2009; Li et al., 2009a; Liu et al., 2009; Ma and Ma,

* Corresponding author at: College of Resources Science and Technology, Beijing Normal University, No. 19, Xinjiekouwai Street, Haidian District, Beijing 100875, China. Tel./fax: +.86 10 58802716
E-mail addresses: zdxzqyzsy@163.com (S.-Y. Zhang), xyli@bnu.edu.cn (X.-Y. Li), myj3648@163.com (Y.-J. Ma), zhaoguoqin2008@126.com (G.-Q. Zhao), lhataki@163.com (L. Li), chenji@ieecas.cn (J. Chen), fhzmjzy@mail.bnu.edu.cn (Z.-Y. Jiang), ymhuang@bnu.edu.cn (Y.-M. Huang).

http://dx.doi.org/10.1016/j.coldregions.2014.02.001
0165-232X/

2006; Ma et al., 2003; Tanaka et al., 2001, 2003; Zhang et al., 2003). These previous studies mostly focused on the meadow, steppe, swamp and shrub ecosystems, whereas little work has been performed on the alpine riparian shrub ecosystems.

Riparian zones are the interfaces between terrestrial and aquatic ecosystems (Gregory et al., 1991; Meehan et al., 1977; Swanson et al., 1982), and it is believed that they will become "hotspots" for climate change adaptation in the 21st century (Capon et al., 2013). Riparian zones are likely to be highly vulnerable to climate change impacts, such as higher temperatures, as well as altered hydrological and ice conditions (Capon et al., 2013; Catford et al., 2013; Nilsson et al., 2013), and can serve as early warning systems of changing environmental conditions (Johnson et al., 2006). Surface energy partitioning and water fluxes in the riparian zone varies seasonally and yearly with the fluctuation of available radiation, temperature, vapor pressure deficit, soil water content and precipitation pattern due to the high climatic variability (Dahm et al., 2002). *ET* by riparian ecosystems is an important component of the watershed water balance in semi-arid and arid regions (Goodrich et al., 2000; Lenters et al., 2011; Scott et al., 2008; Serrat-Capdevila et al., 2011), and it is easily influenced by the fluctuation of the water table (Williams et al., 2006) and freeze–thaw cycle (Zhang et al., 2003). However, observations of water and heat coupling in the field of riparian ecosystems are surprisingly limited (Yang and Chen, 2011).

Myricaria squamosa Desv. is a common but important alpine riparian shrub in the Qinghai–Tibet Plateau and widely distributed in river valleys at an altitude between 2400 and 4600 m. No known studies have been conducted on the ecohydrological processes of *M. squamosa* in any country, although it is also widely distributed in Afghanistan, India, Nepal, Pakistan and other locations throughout the world. The *M. squamosa* community takes up 303.85 km^2 and 1.22% of land area in the Qinghai Lake watershed in the northeastern of the Qinghai–Tibet Plateau. The importance of riparian zones far exceeds their minor percentage of the land base because of their outstanding geographic position within the landscape and the inseparable linkages between terrestrial plant and aquatic ecosystems (Gregory et al., 1991; Mander et al., 1997; Meehan et al., 1977). As one of the constructive shrub species, *M. squamosa* plays a critical role in reducing bank erosion and providing habitat in breeding season for an endemic migratory fish, *Gymnocypris przewalskii*, in Qinghai Lake (Chen et al., 2008; Zhang et al., 2005) but has been seriously degenerated during recent decades due to the overstocking of sheep and yak, along with other anthropogenic activities (Li et al., 2009b). *ET* by *M. squamosa* has not been measured in the region up to now, but such an analysis is very important for the water balance analysis of the Qinghai Lake watershed, just as in other riparian ecosystems in semi-arid region (Goodrich et al., 2000; Scott et al., 2008; Serrat-Capdevila et al., 2011). Qinghai Lake, a closed saline lake, is the largest lake in China. It has experienced severe water level decline during the last 50 years, although a gradual rise occurred during recent years (Li et al., 2007b; Zhang et al., 2011a). The causes of the decline of lake level are believed to mostly be climatic factors (Li et al., 2007b), whereas water consumption by human beings, animals and crop production, industry, along with other human activities, accounts for only 3% of the available fresh water resources in the Qinghai Lake watershed (Yi, 2011), but the role of water consumption in land ecosystems in lake water level fluctuation is not clear, especially for riparian water resources, which are in great demand for use in agriculture, urban development and ecosystem services.

The objectives of this study were (a) to measure surface energy partitioning over *M. squamosa* community, (b) to evaluate temporal variability in *ET* and (c) to analyze the influence of freeze–thaw cycle, soil water content, and groundwater table fluctuation on energy partitioning and *ET*. This study provides valuable information regarding water consumption by the *M. squamosa* community that elucidates the hydrological behavior of alpine riparian ecosystems.

2. Materials and methods

2.1. Site description

This study was conducted in a valley in the lower reaches of the Shaliuhe River, the second largest river in Qinghai Lake watershed, in the northeast region of the Qinghai–Tibet Plateau, China (37°14′N, 100°12′E, 3216 m *a.s.l.*, Fig. 1), which is situated in a semiarid, cold and high-altitude climate zone. The mean annual temperature and precipitation between 1957 and 2006 were −3.3 °C and 378.2 mm, respectively. The winter is clear, dry, and cold, whereas the summer is warm and wet. Approximately, 70–80% of the annual precipitation occurs in summer and autumn.

The experimental site is approximately 8 km away from the Qinghai Lake. The site is 1.4 km^2 in area with a width of approximately 0.7 km, a length of 2 km, and has a flat topography. The soil texture is coarse sand at 0–20 cm, pebble bed with some coarse sand at 20–50 cm, and pebble bed with little coarse sand under 50 cm. The groundwater level fluctuates from 1.5 to 0.5 m within a year. Local wind direction is significantly controlled by lake–land breeze, and the wind mostly blows from lake to land during the day and reverses at night. Seasonal change of wind direction is not distinguished. Wind speed is less than 4 m s^{-1} most of the time. *M. squamosa* shrub is the only dominant overstory species with 60% coverage, approximately 1 m height, and has a leaf area index of 5.78 m^2 m^{-2} in the mid-growing season. Understory vegetation are *Potentilla anserina*, *Logotis brachystachya*, *Lancea tibetica*, and other herbs, with a height of approximately 0.5 m, coverage of 77% and a leaf area index of 5.45 m^2 m^{-2} in the mid-growing season.

2.2. Estimation of ET and energy fluxes using the Bowen ratio energy balance method

The Bowen ratio energy balance (BREB) method was used to estimate actual *ET* by calculating the partition of convective fluxes between latent and sensible heat (Bowen, 1926). The BREB is a micrometeorological method often used to estimate latent and sensible heat flux because of its simplicity, robustness, and low cost (Todd et al., 2000). It is considered to be a fairly robust method and favorably compares with other methods such as weighing lysimeters (e.g., Prueger et al., 1997), eddy covariance (e.g., Alfieri et al., 2009) or water balance (e.g., Malek and Bingham, 1993). Its advantages include straight-forward, simple measurements. It requires no information about the aerodynamic characteristics of the surface of interest. It can integrate latent heat fluxes over large areas of hectares. It can estimate fluxes on fine time scales of minutes and provide continuous, unattended measurements (Todd et al., 2000). The BREB method does have a few well documented limitations, including sensitivity to the accuracy of instruments that measure the air temperature and humidity gradients and energy balance terms, the possibility of discontinuous data when the Bowen ratio approaches −1, the possibility of inconsistency of flux–gradient relationships, and the requirement, common to micrometeorological methods, of adequate fetch to ensure adherence to the assumptions of the method (Perez et al., 1999; Todd et al., 2000). All the same, the BREB method has been applied successfully in wetlands with a homogeneous canopy (Drexler et al., 2004) and many other ecosystems (e.g., Daamen et al., 1999; Dawson, 1996; Domingo et al., 1999; Frank, 2003; Peacock and Hess, 2004; Rohli et al., 2004; Si et al., 2005; Xing et al., 2008; Zhang et al., 2008), including semi-arid steppe (Qiu et al., 2011) and farmland (Todd et al., 2000), as well as a vineyard in an arid desert (Zhang et al., 2008), etc. The BREB method has also been applied successfully to plateau systems (Savage et al., 2009; Staudinger and Rott, 1981; Wang et al., 1996). It is based on the energy balance equation:

$$R_n - G = H + LE \quad (1)$$

where R_n is net radiation; G is ground heat flux; H is sensible heat flux and LE is latent heat flux. The Bowen ratio (β) is the ratio of sensible heat flux

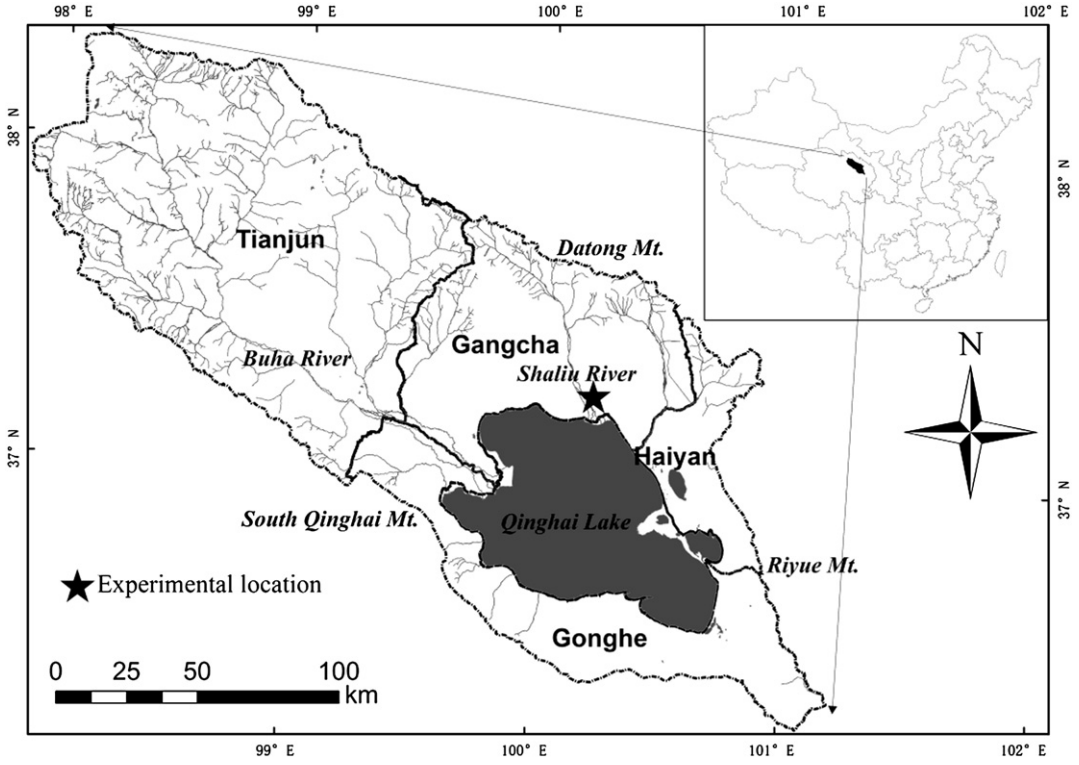

Fig. 1. Location of experimental site in the Qinghai Lake watershed.

to latent heat flux on certain surfaces and can be denoted as a function of the vertical temperature gradient and the humidity gradient. Supposing the eddy water vapor exchange coefficient K_w equals the eddy heat exchange coefficient K_h, viz, $K_w = K_h$, then β can be defined by the following equation (Bowen, 1926):

$$\beta = \frac{H}{LE} = \frac{\rho C_p K_h \frac{\partial T}{\partial z}}{\varepsilon L / P \rho K_w \frac{\partial e}{\partial z}} = \gamma \frac{\Delta T}{\Delta e} \tag{2}$$

where ρ is the air density; C_ρ is the air heat capacity at constant pressure; γ is the psychrometer constant; ε is the ratio of the molecular weight of water vapor to that of dry air; L is the specific latent energy of vaporization; P is the air pressure, and ΔT and Δe are vertical temperature gradient and humidity gradient between the upper and lower air layers, respectively. With the Bowen ratio, LE, H, and ET can be computed separately by using the following equations:

$$LE = \frac{R_n - G}{\beta + 1} \tag{3}$$

$$H = \frac{\beta (R_n - G)}{\beta + 1} \tag{4}$$

$$ET = \frac{LE}{L} = \frac{R_n - G}{L(\beta + 1)}. \tag{5}$$

2.3. Experimental design

A 3-m height Bowen ratio tower was set up over the canopy of *M. squamosa* community at the center of experimental site, and measurements were made between May 2010 and March 2013. The data from each sensor and the corresponding height at which the measurements were made are summarized in Table 1. In particular, two pairs of temperature and humidity probes (HMP45C, Campbell Scientific, USA) were used, and the distance between two temperature–humidity probes has been 0.5 m, as in many former studies (Alfieri et al., 2009; Kar and Kumar, 2007; Qiu et al., 2011; Zhang et al., 2008), which was adequate to measure relative humidity and temperature for the BREB method (Savage, 2010). The fetch requirements for BREB are often

Table 1
Information of meteorological parameters measured at the Bowen ratio tower.

Meteorological parameter	Instrument model, maker	Measurement accuracy	Measurement height (m)
Solar radiation	Model LI-200, Li-Cor, USA	1%	2.6
Net radiation	NR-LITE, Li-Cor, USA	1%	2.6
Air temperature & relative humidity (*RH*)	HMP45C, Campbell Scientific, USA	±0.2 ~ ±0.4 °C, ±2% *RH*	2.0 & 2.5
Soil heat flux	HFP01, Dynamax Inc., USA	5% ~ −15%	−0.05
Wind speed & direction	05103-5, RM-YOUNG, USA	0.25%, ±5 °	2.8
Precipitation	TE525, Texas Electronics, USA	0.25 mm	0.7
Soil temperature	TM10, Dynamax Inc., USA	±0.2 °C	−0.05
Soil moisture	EC-5, Decagon Devices, USA	±3 m^3 m^{-3}	−0.05

suggested to be 100 times the height of the upper sensor (Angus and Watts, 1984; Heilman et al., 1989; Stannard, 1997), whereas Stannard et al. (2004) estimated *ET* at a small wetland using the BREB method with fetch-to-height ratios ranging from 34 to 49 and indicated that estimated errors were small, averaging −1.90 ± 0.59%. Our measurement fetch-to-height ratios were larger than 100 from all directions of the tower. Measurements were taken every 5 s, and the data were recorded every 10 min by a data logger (Model CR1000, Campbell Scientific, USA).

Soil heat flux in the soil was estimated using the following formula (Peacock and Hess, 2004):

$$G = G_{plate} + \frac{\Delta T_s C_s z_s}{\Delta t} \quad (6)$$

where G_{plate} (W m^{-2}) is the soil heat flux measured by the heat flux plates. ΔT_s (°C) is the change in soil temperature between the thermocouples; z_s (0.05 m) is the depth of the soil layer being measured; Δt (600 s) is the time interval, and C_s (MJ m^{-3} °C^{-1}) is the specific heat capacity of soil, estimated from De Vries (1963):

$$C_s = 1.93F_m + 2.51F_o + 4.187F_w \quad (7)$$

where F_m, F_o and F_w are the fractions of mineral, organic matter and water in the soil, respectively. The mineral and organic matter fractions were estimated as 0.40 and 0.15, respectively.

2.4. Screening of data

Inherent errors within the BREB occur when calculated fluxes are not consistent with the flux–gradient relationships. When the temperature and vapor-pressure gradients are in opposite directions, according to the sign of R_n–G, this can lead to calculations of sensible and latent heat fluxes that are inconsistent with the energy balance equation. In this situation, the Bowen ratio method fails, and the data must be discarded. Perez et al. (1999) developed inequalities to identify when the data were inconsistent (Table 2). Data from the BREB will be correct when they fulfill the appropriate inequalities based on the sign of R_n–G and Δe.

Errors also occur when β is close to −1. This causes Eqs. (3)–(5) to tend toward infinity and occurs when the values of latent and sensible heat are of nearly equal magnitude but with opposite signs. This usually happens near sunrise and sunset, due to the small gradients in temperature and vapor pressure and changing flux direction (Ohmura, 1982; Prueger et al., 1997). The range of Bowen ratio around −1 that should be excluded depends on the vapor-pressure gradient and the resolution limits of the sensors. It can be found with an error analysis of β. The excluded interval can be determined using the following equation (Perez et al., 1999):

$$x = \frac{\delta\Delta e - \gamma\delta\Delta T}{\Delta e} \quad (8)$$

Table 2
Conditions used to determine whether heat fluxes are consistent with available energy and vapor pressure differences. R_n is the net radiation, G the surface soil heat flux, Δe the vapor pressure difference between the lower and the upper measurement levels, and LE and H the latent and sensible heat flux, respectively (Perez et al., 1999).

Available energy (R_n–G)	Vapor pressure difference (Δe)	Bowen ratio (β)	Heat fluxes
>0	>0	>−1	$LE > 0$ and $H \le 0$ for $-1 < \beta \le 0$ or $H > 0$ for $\beta > 0$
>0	<0	<−1	$LE < 0$ and $H > 0$
<0	>0	<−1	$LE > 0$ and $H < 0$
<0	<0	>−1	$LE < 0$ and $H \ge 0$ for $-1 < \beta \ge 0$ or $H < 0$ for $\beta > 0$

where $\delta\Delta t$ and $\delta\Delta e$ are the measurement accuracy of HMP45C air temperature and relative humidity sensor from Table 1, respectively, and x is the error interval around −1. The interval of β values, $-1 - |x| < \beta < -1 + |x|$, is excluded.

2.5. Reference ET

The FAO–Penman–Monteith equation was used to estimate daily reference evapotranspiration (ET_r) using the following equation (Allen et al., 1998):

$$ET_r = \frac{0.408\Delta(Rn-G) + \gamma(900/(T+273))u_2(e_s-e_a)}{\Delta + \gamma(1+0.34u_2)} \quad (9)$$

where R_n is the net radiation (MJ m^{-2} day^{-1}); G is the soil heat flux density (MJ m^{-2} day^{-1}); T is the air temperature at 2 m height (°C); u_2 is the wind speed at 2 m height above shrub canopy (m s^{-1}); e_s is the vapor pressure of the air at saturation (kPa); e_a is the actual vapor pressure (kPa); Δ is the slope of the vapor pressure curve (kPa °C^{-1}), and γ is the psychometric constant (kPa °C^{-1}).

3. Results and discussion

3.1. Temporal variation of environmental variables

Meteorological observations at the experimental site (Fig. 2) indicated that the mean daily air temperature was −0.03 °C with a maximum of 17.1 °C and a minimum of −20.6 °C, which suggested that the important features of the local climate were cold, large range of temperature variation and short vegetation growing seasons (May–September). The mean daily relative humidity was 60% with a minimum of 19% and a maximum of 92%. Daily soil temperature was 2.4 °C with a maximum of 14.7 °C and a minimum of −10.7 °C. Daily soil water content was 0.12 m^3 m^{-3} with a maximum of 0.44 m^3 m^{-3} and a minimum of 0.02 m^3 m^{-3}. Daily solar radiation was 204 W m^{-2} ranging from −47 to 385 W m^{-2}. Precipitation was 327 mm, 329 mm and 323 mm in 2010 (May–December), 2011 and 2012, respectively, at the study site.

3.2. Characteristics of the temporal variability of evapotranspiration

Seasonal and annual *ET* and the meteorological variables are shown in Table 3. On an annual basis, the cumulative *ET* was 390 mm and 503 mm in the periods of 2010–2011 and 2011–2012, respectively (Table 3). *ET* fluctuated greatly between years (Table 3), which is common for ecosystems on the Qinghai–Tibet Plateau (Gu et al., 2008; Hu et al., 2009; Li et al., 2013). The *ET* of *M. squamosa* shrubs was less than that of a swamp meadow (Hu et al., 2009) and was not greatly different from shrub-meadow and meadow-steppe (Gu et al., 2008; Hu et al., 2009; Li et al., 2013). However, the cumulative *ET* of *M. squamosa* shrubs exceeded precipitation by approximately 12% (Table 3), which is different from that observed with alpine meadows (Gu et al., 2008), where a previous study indicated that annual *ET* was only approximately 60% of the annual precipitation. Higher annual *ET* than annual precipitation indicates that the riparian shrub ecosystem was a water consumption area, and there were other water sources in addition to local precipitation for this ecosystem, which was in agreement with the results of Zhao et al. (2013), who reported that *M. squamosa* mainly used groundwater and water from the river stream in June and July.

The growing season *ET* from May to September occupied 86% of annual *ET*, whereas the non-growing season *ET* from October to next April only occupied 14%. The high percentage of *ET* in the growing season was similar to the results of Li et al. (2013) and Gu et al. (2008), who reported that more than 80% *ET* of meadows on the Qinghai–Tibet Plateau occurred in growing season from May to September. The growing season

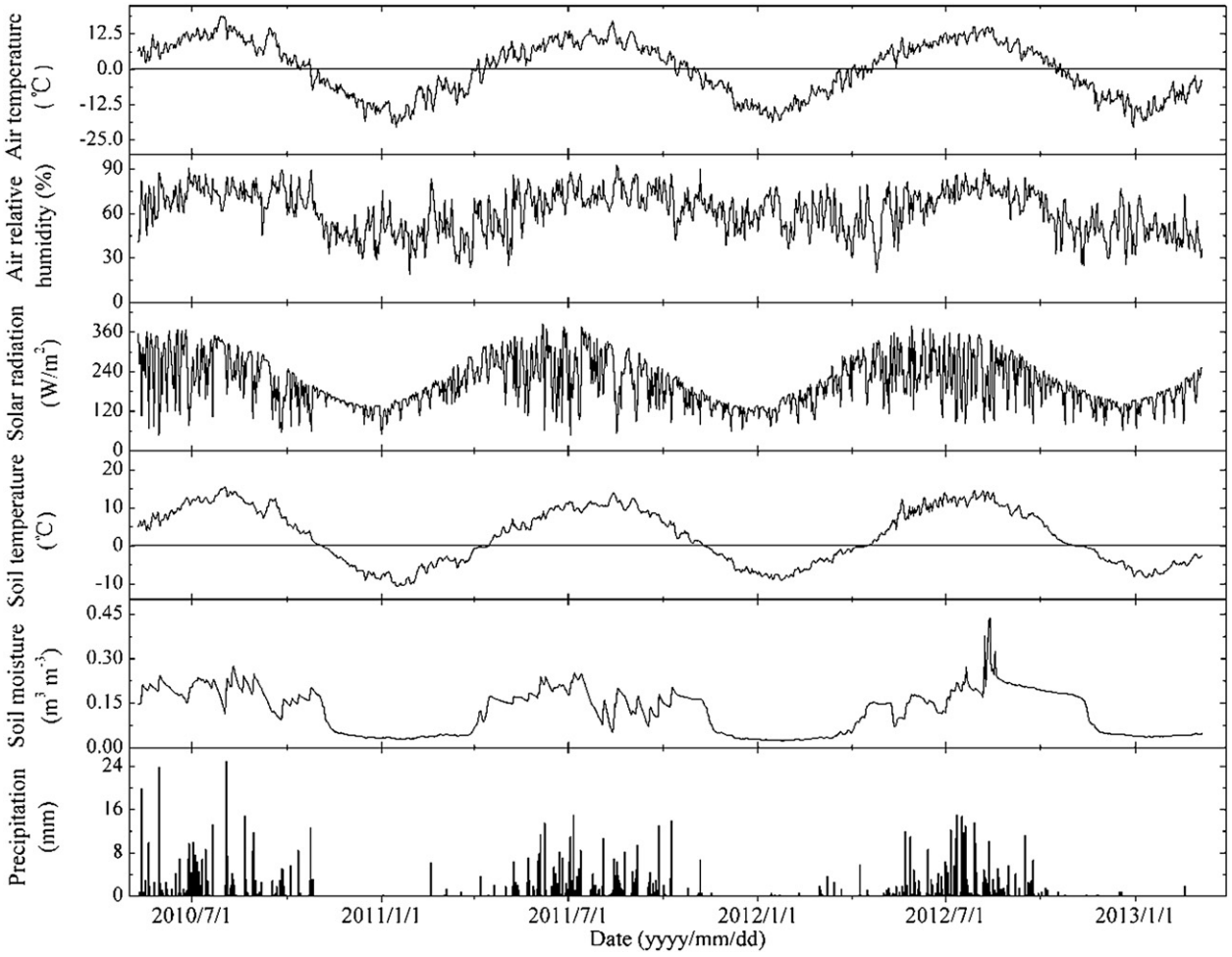

Fig. 2. Daily time series of air temperature, air relative humidity, solar radiation, precipitation and soil temperature and moisture.

ET of *M. squamosa*, averaging 344 mm for three years, was lower than the 807 mm *ET* of swamp meadows (Hu et al., 2009) and higher than the 298 mm *ET* of alpine Qinghai spruce (*Picea crassifolia*) ecosystem (Tian et al., 2011) but was not greatly different from that of alpine shrub-meadow and meadow-steppe estimated by Gu et al. (2008) and Hu et al. (2009), who estimated a growing season *ET* of 290 to 453 mm.

Seasonal variations in daily *ET* and daily reference *ET* from May 2010 to March 2013 are shown in Fig. 3. *ET* displayed a gradual increase from middle April because daily air temperature and soil temperature rose above 0 °C, and the frozen soil began to thaw. The *ET* in May was around 1.0 mm d^{-1}. During the period from June to August, the net radiation and precipitation rose to the peak of the year, and the shrub and understory herb grew luxuriantly, leading to a peak period of *ET*. The maximum daily *ET* was 7.2 mm d^{-1} on July 17, 2011. After September, *ET* decreased quickly due to the decrease of net radiation and the senescence of vegetation. From late October to the following mid-April, the air temperature and soil temperature were under 0 °C, and *ET* remained at a very low level, around 0.3 mm d^{-1}, with a minimum *ET* of −0.4 mm d^{-1} on November 9, 2012. The daily *ET* extent in this study is similar to a *Phragmites australis*-dominated wetland in the Republican River watershed in the USA with similar weather condition, where the maximum daily *ET* was 5.0–8.2 mm d^{-1} and minimum daily *ET* was −1.3 mm d^{-1} (Burba et al., 1999; Lenters et al., 2011; Peacock and Hess, 2004). The seasonal pattern of *ET* was consistent with other ecosystems on the Qinghai–Tibet Plateau (Yao et al., 2008; Zhou et al., 2008).

Table 3
Annual and seasonal ratio of latent (*LE*) and sensible (*H*) heat flux and net radiation (R_n), Bowen ratio (β), and ratio of evapotranspiration (*ET*) and total precipitation (*PPT*) and reference evapotranspiration (ET_r).

Periods	LE/R_n	H/R_n	β	ET/PPT	ET/ET_r
May 2010–Sept. 2010	0.50	0.46	0.91	1.22	0.80
Oct. 2010–Apr. 2011	0.08	1.02	12.59	0.68	0.12
May 2010–Apr. 2011	0.35	0.66	1.87	1.14	0.55
May 2011–Sept. 2011	0.61	0.37	0.61	1.45	0.94
Oct. 2011–Apr. 2012	0.24	0.87	3.65	1.86	0.37
May 2011–Apr. 2012	0.48	0.55	1.16	1.51	0.73
May 2012–Sept. 2012	0.37	0.62	1.68	0.89	0.58
Oct. 2012–Mar. 2013	0.21	0.90	4.34	5.56	0.28
May 2012–Mar. 2013	0.32	0.70	2.16	1.02	0.50
May 2010–Mar. 2013	0.38	0.64	1.67	1.23	0.60

The annual mean ET/ET_r was 0.60, indicating that cumulative *ET* was lower than cumulative ET_r, especially during the non-growing season (Table 3, Fig. 3c). In the earlier growing seasons (at the beginning of May), *ET* was approximately 25% of ET_r. During the mid-growing season in August, daily *ET* values were higher than ET_r by approximately 15%. Similar to our results, for *P. australis*-dominated wetland, Burba et al. (1999) reported *ET* was 30% higher than ET_r during the mid-growing season. Toward the end of the season, *ET* was approximately 33% of ET_r. During the frozen season, *ET* was as low, approximately 3% of ET_r. The rise of *ET* in May is thought to be the result of the thaw, whereas the peak of *ET* from June to August was the result of the increase of R_n, precipitation and vegetation growth (Yao et al., 2008; Zhang et al., 2003). In winter and spring, the frozen soil expanded, so water was coagulated and could not move freely as liquid water. The lowest available liquid water for evaporation led to the lowest *ET* (Zhang et al., 2003).

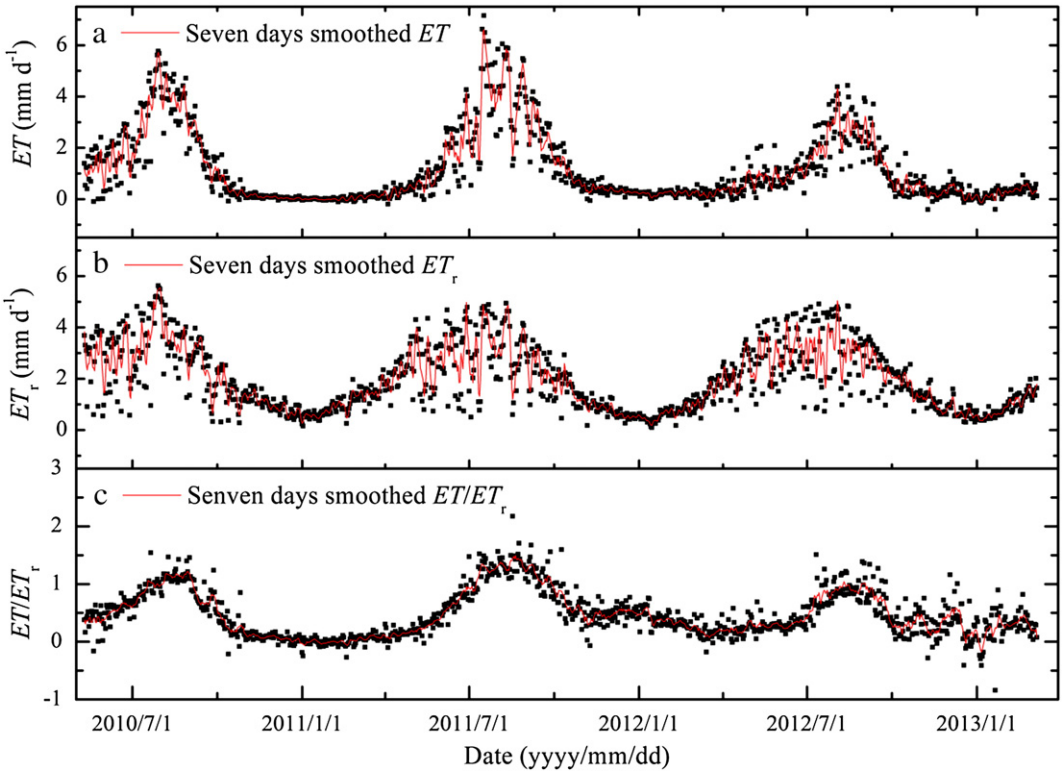

Fig. 3. The variation of the daily evapotranspiration (*ET*), reference evapotranspiration (ET_r) and the ratio of *ET* to ET_r (ET/ET_r) from May 2010 to March 2013.

Throughout the day, when clear, cloudless conditions prevailed, the *ET* rate varied significantly (Fig. 4). In winter, the *ET* rate was very small, daily *ET* was nearly zero (Fig. 4a). In April, the *ET* rate began to rise around 8:00 and rose to approximately 2.0 mm d^{-1} at 13:00 then returned to near zero at 18:00. No *ET* occurred at night, when the *ET* rate frequently dropped below zero. The daily *ET* was 0.34 mm on April 22, 2011 (Fig. 4b). In July, the *ET* rate began to rise around 7:00 and rose to approximately 19.2 mm d^{-1} at 13:00 then dropped to lower than 1.0 mm d^{-1} at 19:00. No *ET* occurred after midnight, when the *ET* rate frequently dropped below zero. Daily *ET* was 6.15 mm on July 22, 2011 (Fig. 4c). The *ET* rate scene in October was similar to that in April except that the *ET* rate at midday was higher in October, and the daily *ET* was 1.01 mm (Fig. 4d).

According to the stepwise multiple regression between *ET* and meteorological variables (Table 4), *ET* rates were found to be coupled to different variables in different periods (Table 5). In the frozen winter (January, February and December), T_{smin} played the most important role in *ET* variation because it has the largest absolute standardized coefficient, indicating that *ET* was limited by temperature. In the thawing period (March and April), *ET* rates were found to be closely coupled to *VPD*, as there was rarely precipitation in the preceding winter and this period (Fig. 2). In the growth season (between May and September), *ET* variation was mostly driven by R_n, the same with a *P. australis*-dominated wetland in the Republican River basin of south-central Nebraska (USA) (Lenters et al., 2011). Former results have also indicated that the *ET* on the Qinghai–Tibet Plateau was controlled by R_n, especially in the growing season (Liu et al., 2010). In the freezing period (October and November), *ET* was controlled by R_n and T_{smax}. For all periods, T_s was the key variable controlling *ET* rates. In general, temperature and net radiation were the key variables controlling daily *ET* rates in this alpine riparian shrub. Our results are different from those of previous studies, many of which have reported that *VPD* and *SWC* were the most important environmental factors affecting *ET* (Alfieri et al., 2007; Cavanaugh et al., 2011; Domingo et al., 1999; Li et al., 2007a; Yoshida et al., 2010), whereas *VPD* only played the most important role in the thawing period and a common role in the growing period and the entire period. *SWC* played some roles in the frozen period, growing period and the entire period. Compared with *VPD* and *SWC*, T_s played a more important role as its influence was only lacking in the thawing period. Along with the synchronous fluctuation with radiation, T_a and precipitation (Fig. 2), higher T_s has been verified to increase *ET* (Feldhake and Boyer, 1986).

3.3. The characteristics of energy partitioning

The diurnal variation in the magnitude of *H* on a typical clear winter day (January 22, 2011) closely followed that of R_n (Fig. 4a). Rises, peaks, drops in the two parameters occurred concurrently. The value of *H* rose from −31.1 to 339.5 W m^{-2} between 8:00 and 13:00 and then *H* declined steadily to 4.6 W m^{-2} until 17:00. Nocturnal values of *H* changed from −63.5 W m^{-2} at 18:00 to −33.0 W m^{-2} at 7:00 of the next day. On the same day, *G* was positive only at 13:00 to 18:00, with a maximum of 13.1 W m^{-2} at 15:00. The values of *G* at most times of this day were negative, with a minimum of −20.9 W m^{-2} at 6:00, indicating that the heat storage term was an important source of energy in winter. On the same day, daytime *LE* was quite low, ranging from −10.44 to 4.3 W m^{-2}, with a mean value of −0.1 W m^{-2}.

In spring, on April 22 (Fig. 4b), the maximum of R_n and *H* was 550.9 and 462.1 W m^{-2}, respectively. The rise and stabilization of *H* were 1 h ahead and after that of January 22. The positive value of *G* began from 9:00 and ended at 21:00 with a maximum of 31.7 W m^{-2} at 15:00 and a minimum of −13.6 W m^{-2} at 6:00. The *LE* was relatively low in this period, ranging from −31.7 to 62.7 W m^{-2} with a mean value of 9.9 W m^{-2}.

In summer, on July 22 (Fig. 4c), the maximum of R_n was 710.6 W m^{-2}. In this period, the *LE*, with a maximum of 548.5 W m^{-2}, accounted for the major part of the R_n and fluctuated following the pattern of R_n. The diurnal values of *H* between 10:00 and 17:00 had not conspicuously peaked but ranged from 61.6 to 168.8 W m^{-2}. The mean and maximum of *G* were 4.9 and 31.7 W m^{-2}, respectively, indicating that the soil

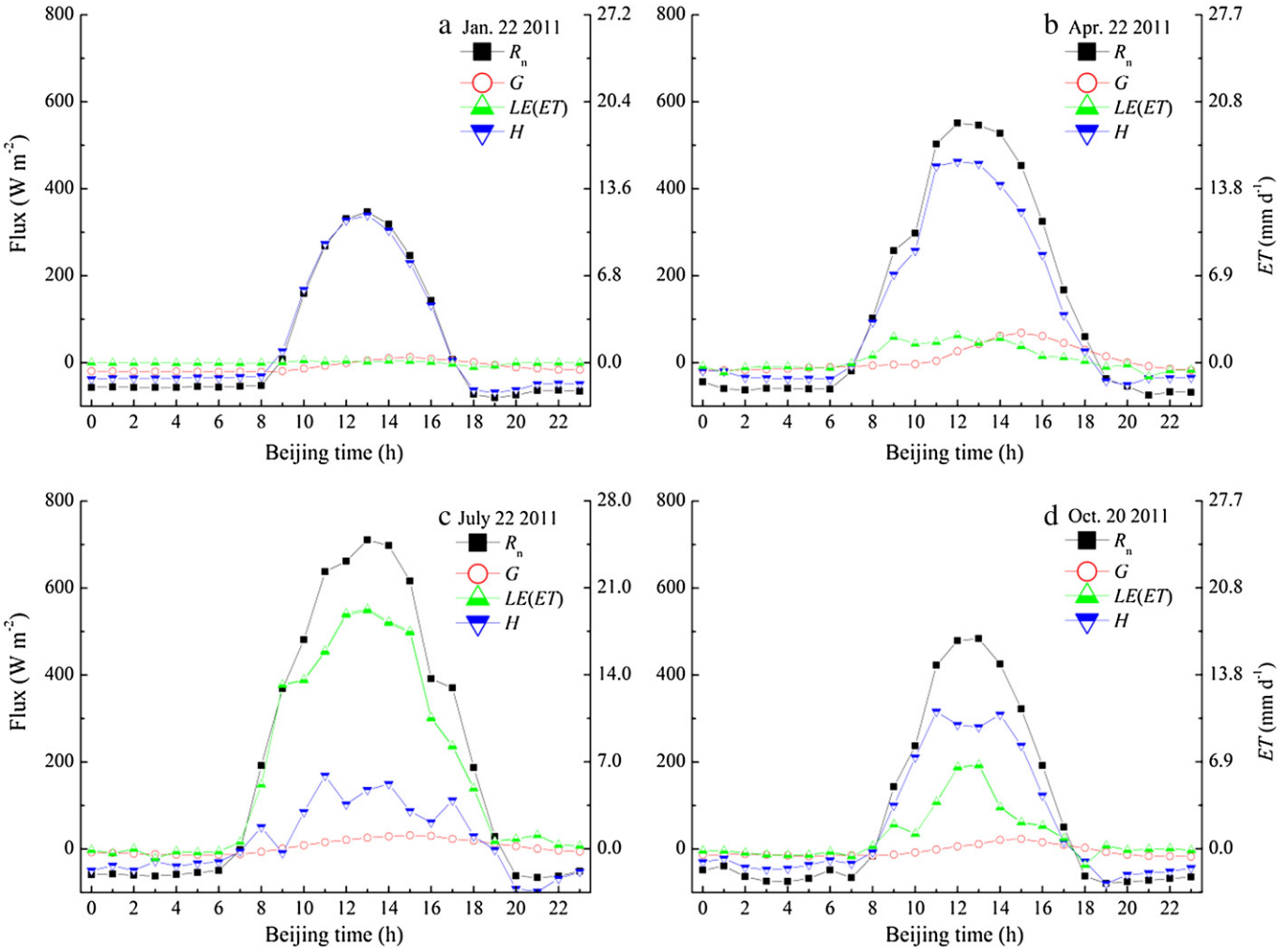

Fig. 4. Seasonal variation of diurnal net radiation flux (R_n), latent heat flux (LE), evapotranspiration (ET), sensible heat flux (H), and soil heat flux (G) of the clear days.

stored the heat from radiation between 9:00 and 21:00 when the G was positive.

In autumn, on October 20 (Fig. 4d), the maximum of R_n was 483.6 W m^{-2}, a bit lower than that on April 22. In this period, H accounted for the major part of the net radiation expenditure again. However, in the middle of the daytime, from 11:00 to 14:00, the LE took approximately 32.2% of the net radiation expenditure, more than that on April 22, whereas the H decreased in this period. The positive value of G lasted from 12:00 to 18:00, and the mean and minimum of G were −5.5 and −17.5 W m^{-2}, respectively, indicating that the heat storage term was the source of energy in this period. In general, the hourly fluctuation of energy fluxes within a day followed mostly the pattern of energy input (R_n), but each section was a different percentage in different seasons, just was similar to the results of a meadow ecosystem also on the Qinghai–Tibet Plateau (Gu et al., 2005) or a *P. australis*-dominated wetland in the Republican River basin of south-central Nebraska (USA) (Lenters et al., 2011).

Seasonal variations in the daily H during the three years are examined in Fig. 5a. Peak values of daily H (between 100 and 130 W m^{-2}) occurred during May before the rapid growth of plants. H decreased rapidly following plant outgrows each year. At the end of the growth period, H reached another peak, approximately 70 to 100 W m^{-2}. The minimum daily H (between 10 and 30 W m^{-2}) occurred during December when the net radiation is the lowest. However, the negative daily total sensible heat fluxes were observed during rainy days, reaching up to −10 W m^{-2}.

Seasonal variations in total daily G during the three study years are examined in Fig. 5b. Before the end of March, G was negative, indicating that the heat flux direction was from the soil to air. Between early April and mid-September, G was positive except for some rainy days, indicating that the heat flux direction was from the air to soil. The negative G corresponding to heavy precipitation events was also reported by Tanaka et al. (2003). From mid-September to the end of March in the next year, G was negative. The direction changes of ground heat flux were in accord with the gradients of soil temperature and air temperature (Fig. 2). The maximum of the daily ground heat flux was between 19 and 26 W m^{-2} and the minimum between −16 and −13 W m^{-2}.

Table 4
Variables evaluated in stepwise multiple regressions. During each iteration, variables with a probability of a type II error >0.1 ($p >$ 0.1) were removed from the analysis.

Variables	Units	Definition
R_n	W m^{-2}	Net radiation
G	W m^{-2}	Ground heat flux
e_a	kPa	Air water vapor pressure
VPD	kPa	Vapor pressure deficit
T_a	°C	Air temperature
T_s	°C	Soil temperature
WS	m s^{-2}	Wind speed
SWC	m^3 m^{-3}	Soil water content
PPT	mm	Precipitations
T_{amax}	°C	Daily maximum air temperature
T_{amin}	°C	Daily minimum air temperature
T_{smax}	°C	Daily maximum soil temperature
T_{smin}	°C	Daily minimum soil temperature

Table 5
Results of stepwise multiple regression model of *ET* and micro-meteorological conditions.

Dependent variable	Periods (months)	Variables entered	Coefficients		Standardized coefficients	*F*	R^2
			B	Std. error			
ET	1, 2, 12	(Constant)	1.74	0.16		31.99	0.50*
		T_s	−0.16	0.03	−1.79		
		e_a	−2.56	0.32	−0.71		
		SWC	−14.34	1.66	−0.61		
		WS	−0.045	0.010	−0.23		
		T_{smin}	0.22	0.03	2.85		
		R_n	0.0030	0.0005	0.37		
		G	−0.019	0.004	−0.43		
		T_a	0.024	0.005	0.56		
	3, 4	(Constant)	−0.11	0.06		32.72	0.33*
		VPD	0.57	0.12	0.41		
		R_n	0.0023	0.0008	0.26		
	5, 6, 7, 8, 9	(Constant)	−1.58	0.45		209.15	0.81*
		G	−0.058	0.007	−0.33		
		R_n	0.017	0.001	0.66		
		T_{smin}	0.21	0.04	0.48		
		T_{smax}	−0.11	0.01	−0.26		
		SWC	−2.47	0.67	−0.09		
		VPD	3.49	0.80	0.41		
		e_a	2.65	0.81	0.45		
		WS	−0.14	0.05	−0.06		
		T_a	−0.17	0.08	−0.41		
	10, 11	(Constant)	0.15	0.05		50.10	0.36*
		R_n	0.0048	0.0012	0.33		
		T_{smax}	0.040	0.010	0.33		
	All	(Constant)	−2.01	0.12		739.24	0.87*
		e_a	2.92	0.14	0.86		
		R_n	0.014	0.001	0.65		
		G	−0.046	0.003	−0.30		
		T_{smax}	−0.19	0.01	−1.21		
		VPD	2.98	0.21	0.40		
		T_{amax}	−0.024	0.010	−0.17		
		T_s	0.27	0.02	1.60		
		T_a	−0.10	0.01	−0.81		
		SWC	−1.25	0.38	−0.08		

* Significant at the 0.01 level.

The average contribution of latent heat flux, ground heat flux and sensible heat flux to the energy budget was calculated for each month (Fig. 6). The average annual values are approximately 60% of net radiation used in sensible heat flux and 40% used in latent heat flux in the three study years. This demonstrates the importance of sensible heat flux in the energy balance at this site. The latent heat flux is larger than sensible heat flux only at July, August and September, partly due to the short growth period. The monthly mean *G* is positive only in April, May, June and July. In November, December and January, when net radiation is the lowest in the year, *G* can take 25–61% of net radiation, which demonstrates the importance of ground heat flux in the energy balance at this site in winter.

The observed seasonal patterns of energy partitioning at this alpine riparian shrub were similar to other locations on the Qinghai–Tibet Plateau (Gu et al., 2005; Tanaka et al., 2003), but *H* began to increase later, and the *G* dropped below zero earlier than the *Kobresia humilis* alpine meadow (Gu et al., 2005). The *LE* of alpine riparian shrub took more of R_n than that of the *K. humilis* alpine meadow during the growth period (Gu et al., 2005; Li et al., 2013). The *LE* of alpine riparian shrub took approximately 50% of R_n between May and September, with a

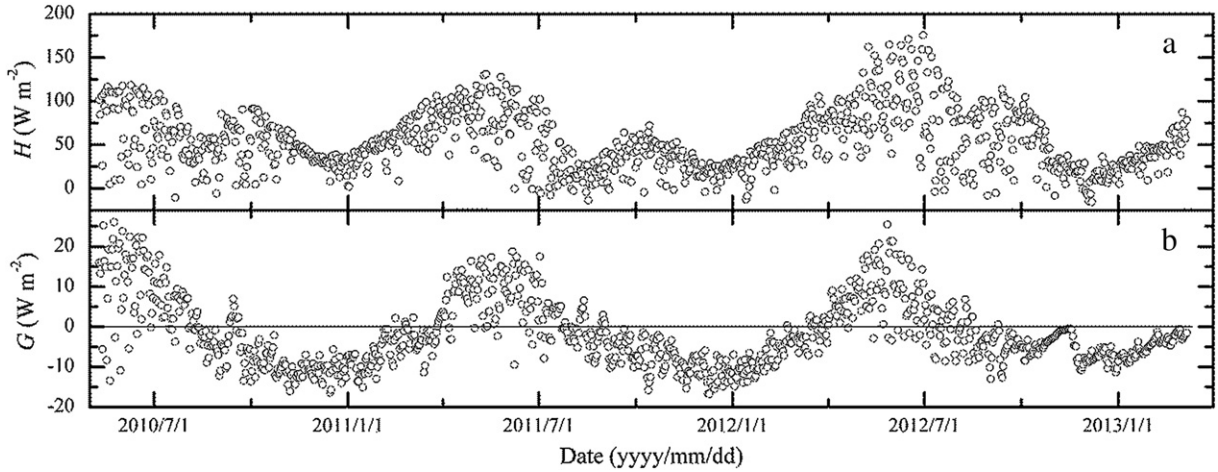

Fig. 5. The variation of daily sensible heat flux (*H*) and ground heat flux (*G*) from May 2010 to March 2013.

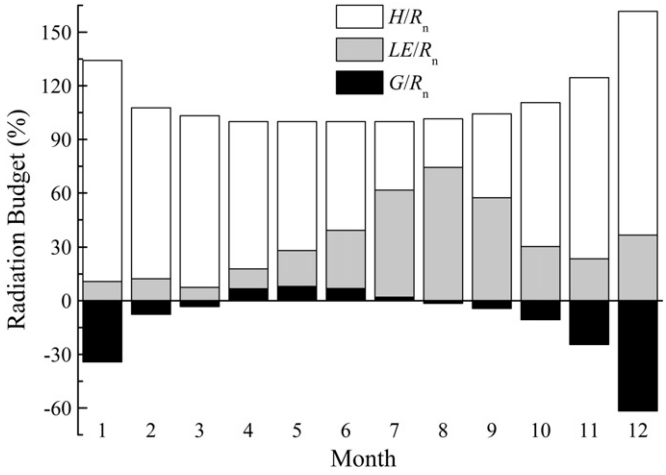

Fig. 6. The monthly variation of the ratio of sensible heat flux (*H*), latent heat flux (*LE*), ground heat flux (*G*) to the net radiation (R_n).

maximum of 75% in August, whereas the *LE* of alpine meadow took approximately 44% of R_n with a maximum of 53% of R_n (Gu et al., 2005; Li et al., 2013). These results indicate that more energy was consumed by *LE* in riparian ecosystems than in alpine meadow ecosystems.

3.4. Effects of freezing and thawing on ET and energy partitioning

To analyze the effects of soil thawing on *ET* and energy partitioning, clear days between February and April 2011 were chosen as the study period. The daily maximum air temperature above 0 °C appeared on the 34th day of year (February 3), and soil at 5 cm depth began to thaw at approximately the 89th day of year (March 30) and completely thawed on the 107th day of year (April 17). Before the soil thawed, viz. minimum soil temperature (T_{smin}) was less than 0 °C. The β was large, and e_a, *SWC* and *ET* remained at a low level. With the increase of T_{smin}, the *G* become positive and *SWC* increased quickly before T_{smin} was over 0 °C. After the soil thawed, viz. T_{smin} was larger than 0 °C, and the β dropped, and *ET* increased quickly with T_s increases (Fig. 7). These results indicate that the soil thawing came along with soil heat fluxes turning positive, and thawing increased *SWC*, e_a, and *ET*. After the soil thawed, more R_n was transferred to *LE*.

To analyze the effects of soil freezing on *ET* and energy partitioning, clear days between September and December 2011 were chosen as the study period. The first daily minimum air temperature below 0 °C appeared on the 251th day of year (September 8, 2011), and a T_{smin} below 0 °C appeared on the 316th day of the year (November 12, 2011), whereas the soil liquid water content decreased to a stable low level on the 326th day of the year (November 22, 2011). Before the soil was frozen, the *G* was negative. *G*, e_a, and *VPD* decreased with T_{smin} decrease (Fig. 8). The β increased and *ET* decreased substantially as T_{smin} slid toward 0 °C (Fig. 8). When soil was freezing, the tendency of *G*, e_a, and *VPD* did not change significantly, whereas β remained at a high level, and *ET* remained at a low level (Fig. 8). The results indicate that the soil being frozen limited the *ET*, increased β and transferred more R_n to *H*.

Former studies indicate that freezing and thawing have important influence on the *ET* and surface energy fluxes (Gu et al., 2005; Yao et al., 2008; Zhang et al., 2003). Frozen soil thawing can create a strong heat sink that reduces surface temperature and therefore *H* (Eugster et al.,

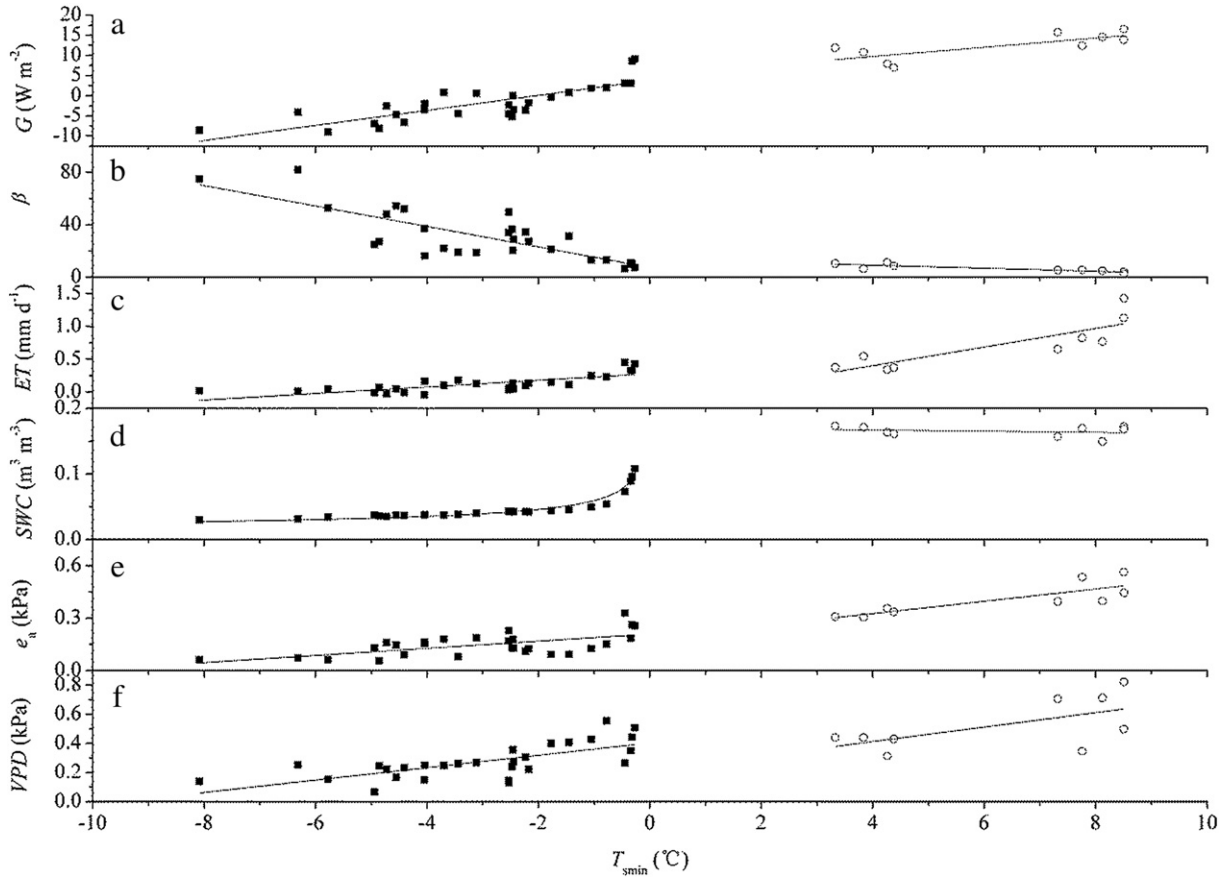

Fig. 7. Relationship between daily soil heat flux (*G*), Bowen ratio (β), evapotranspiration (*ET*), soil liquid water content (*SWC*), water vapor pressure (e_a), vapor pressure deficit (*VPD*) and minimum soil temperature (T_{smin}) of clear days between February and April, 2011.

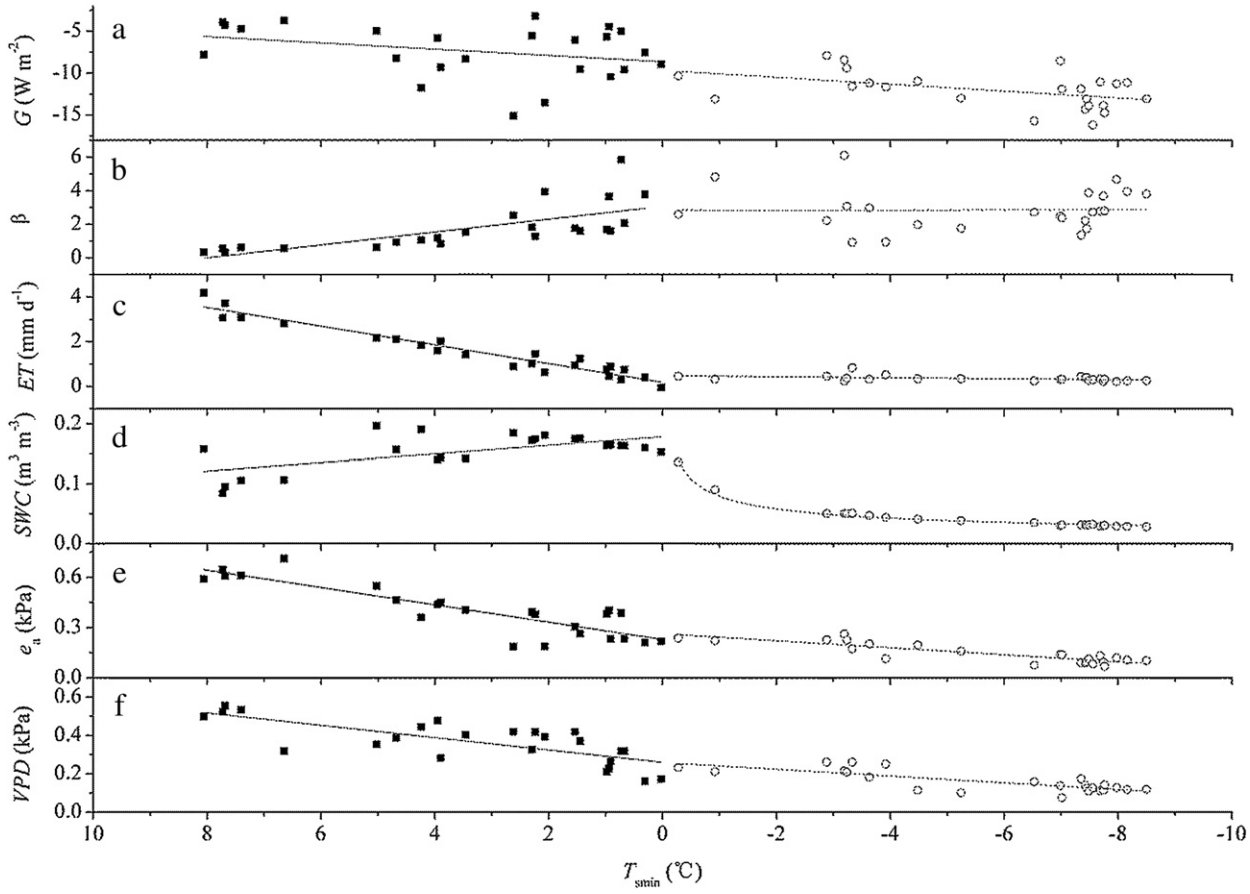

Fig. 8. Relationship between daily soil heat flux (G), Bowen ratio (β), evapotranspiration (ET), soil liquid water content (SWC), water vapor pressure (e_a), vapor pressure deficit (VPD) and minimum soil temperature (T_{smin}) of clear days between September and December, 2011.

2000), whereas frozen soil can retain soil water during the frozen period, so the high SWC can be present after thawing and therefore relatively high ET (Yang et al., 2002; Zhang et al., 2003). These processes are believed to play an important role in the seasonal shift in the Qinghai–Tibet Plateau (Yang et al., 2002). Considering the significant warming trend and the dramatic ground surface warming and therefore its significant influence on the freeze–thaw cycle (Wu et al., 2013; You et al., 2010), climate warming would have great impact on the local and regional ET and surface energy partitioning, e.g., earlier onset of the non-frozen season generally promotes annual ET (Zhang et al., 2011b).

3.5. Effects of groundwater, precipitation and soil water content on evapotranspiration and energy partitioning

Groundwater is considered to have an important effect on the ET of riparian ecosystems. Elevated total ET rates in the monospecific *Tamarix* shrub associated with flooding were found by Cleverly et al. (2006). In

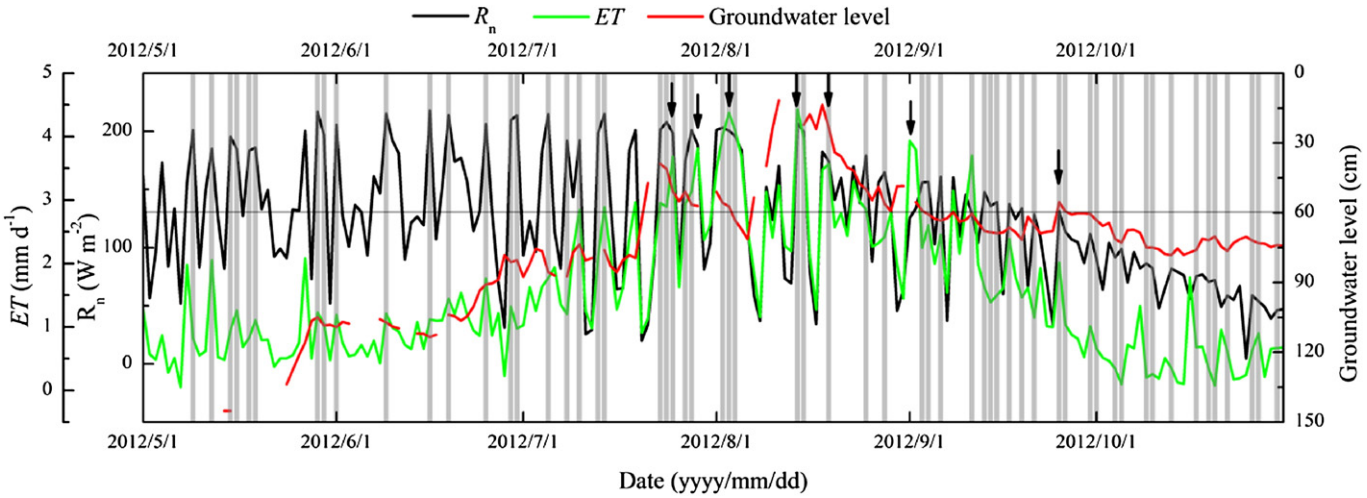

Fig. 9. Fluctuation of net radiation (R_n), evapotranspiration (ET) and groundwater level. The gray background indicates clear days.

this study, similar effects were observed as shown in Fig. 9. When the ground water level was lower than 60 cm, a rise of groundwater level could elevate the *ET* rates. These results can be explained by the results of Zhao et al. (2013), who found that the roots of *M. squamosa* are mainly distributed at 0–60 cm of the soil profile, and *M. squamosa* mainly used ground water and river water in June and July, but soil water in August and September. Thus, when the groundwater level reached the main root zone, soil water content at 0–60 cm would increase sharply, and *M. squamosa* grew quickly, resulting in the increase in the *ET* rate.

ET rates usually varied with the fluctuation of R_n, and precipitation decreased *ET*, *H* and *G*, through shading and the resulting reduction in R_n (Fig. 10), the same as the results of Cleverly et al. (2006) in a *Tamarix* ecosystem. Low soil water content limited *ET* in the frozen period as shown above. During the growing period, continuous sunny days or rain pulses could alter the *ET* and energy flux patterns. During sunny days from July 27 to August 1, 2010, the net radiation and ground heat flux changed little, but the latent heat flux decreased, and the sensible heat flux increased (Fig. 10). The decrease of *ET* and the change of energy partition were connected to the decrease of soil water content (Fig. 10). After a long period of drought, a rain pulse could increase *ET* sharply. Two 24.9 mm and 7.4 mm rain events occurred on August 3 and 4, 2010, and then on August 5 and 6, 2010, the *LE* increased and the sensible heat flux decreased, although the R_n was almost the same (Fig. 10). These results indicate that *SWC* was an important factor controlling *ET*. This is partly due to the coarse texture soil property, as the capillary water could not reach the ground surface for soil evaporation in periods of drought (Wang, 2003).

4. Conclusions

This study is the first report describing *ET* and surface energy partitioning over a *M. squamosa* riparian shrub community, which is widely distributed on the Qinghai–Tibet Plateau. Annual *ET* was generally greater than local precipitation, indicating that the *M. squamosa* riparian shrub community is a water consumption area of the Qinghai Lake watershed. The growing season *ET* was over 80% of annual *ET*, and the *ET* in the non-growing season was quite low due to the long frozen period, which limited soil water loss from the soil surface. Cumulative *ET* was lower than cumulative ET_r, especially in the frozen period. In general, soil temperature played a key role in daily *ET* rates in these alpine riparian shrub ecosystems.

Annual sensible heat flux covered 60% of net radiation and latent heat flux covered 40%. *LE* was responsible for the main part of R_n from July to September, whereas *H* was the highest in May and June and lowest in late September and early October. *G* was positive only from April to mid-September, and it is an important heat source of surface in winter and spring.

As an alpine riparian ecosystem in semi-arid region, *ET* and energy partitioning of *M. squamosa* community were affected by the freeze–thaw cycle, groundwater fluctuation, precipitation pulses and *SWC*.

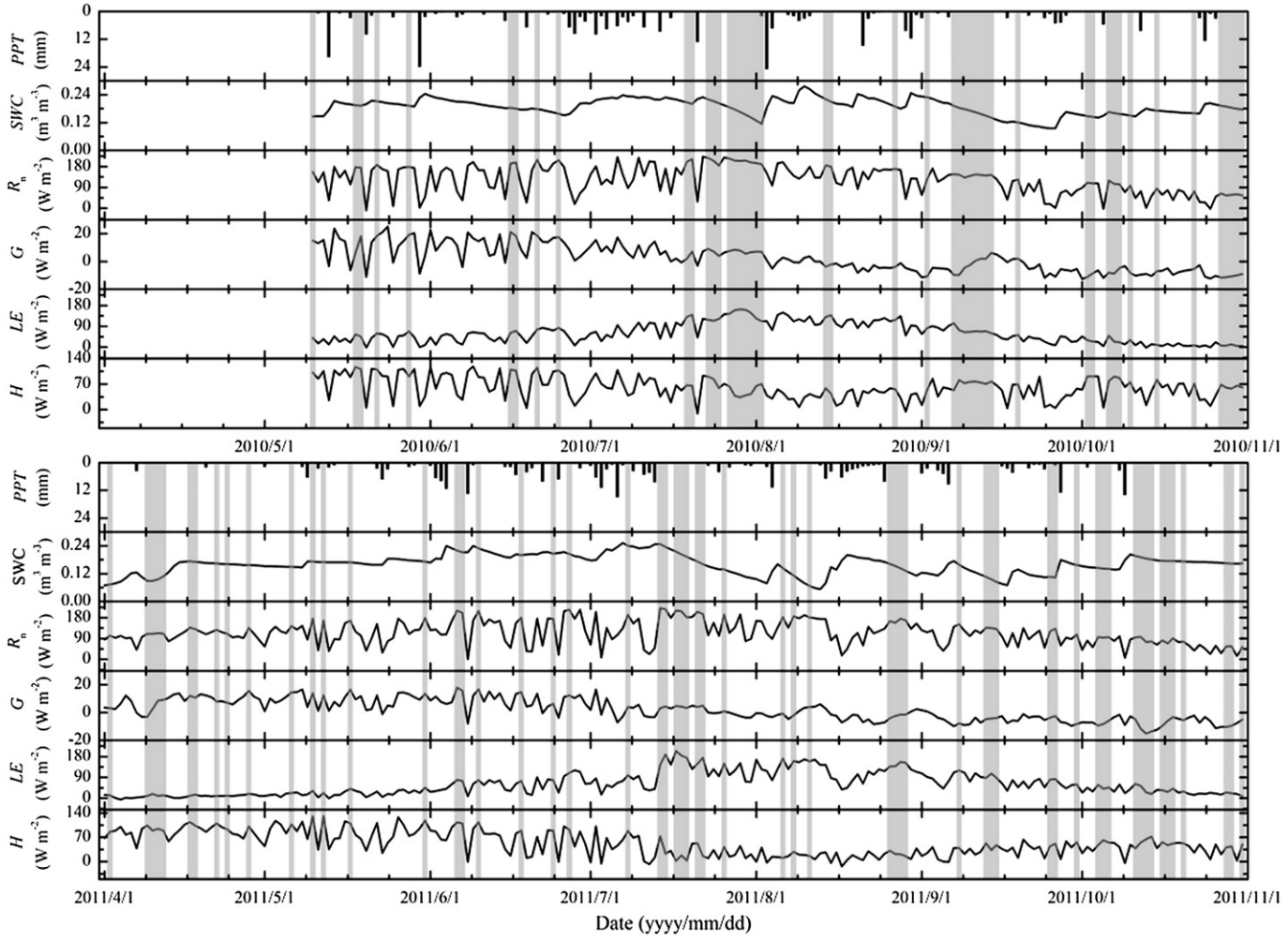

Fig. 10. Daily precipitation (*PPT*), soil liquid water content (*SWC*), net radiation (R_n) soil heat flux (*G*), latent heat flux (*LE*), and sensitive heat flux (*H*) during May 2010 and December 2011. The gray background indicates clear days.

Considering the warming climate, the increased temperature might affect the freeze–thaw cycle and therefore the soil water content pattern and groundwater fluctuation.

Climate warming would result earlier onset of the non-frozen season and longer growing season. Considering the significant influences of temperature, freeze–thaw cycle on the *ET* of the riparian shrub ecosystem and its available of river water and groundwater, our results indicate that climate change could have an important impact on the local *ET* and surface energy partitioning, whereas in turn, different surface energy partitioning patterns would influence the local and regional climate.

Acknowledgments

We would like to thank the editors and two anonymous reviewers for valuable and constructive comments. The study was financially supported by the National Science Foundation of China (NSFC 41130640, 41025001, 41390462 and 41321001), the Fundamental Research Funds for the Central Universities, the PCSIRT (No. IRT1108), and projects from the State Key Laboratory of Earth Surface Processes and Resource Ecology.

References

Alfieri, J.G., Blanken, P.D., Yates, D.N., Steffen, K., 2007. Variability in the environmental factors driving evapotranspiration from a grazed rangeland during severe drought conditions. J. Hydrometeorol. 8 (2), 207–220.

Alfieri, J.G., Blanken, P.D., Smith, D., Morgan, J., 2009. Concerning the measurement and magnitude of heat, water vapor, and carbon dioxide exchange from a semiarid grassland. J. Appl. Meteorol. Climatol. 48 (5), 982–996.

Allen, R.G., Pereira, L.S., Raes, D., Smith, M., 1998. Crop Evapotranspiration—Guidelines for Computing Crop Water Requirements—FAO Irrigation and Drainage Paper 56. FAO, Rome, Italy.

Angus, D.E., Watts, P.J., 1984. Evapotranspiration—how good is the Bowen ratio method? Agric. Water Manag. 8 (1–3), 133–150.

Betts, A.K., Ball, J.H., Viterbo, P., 1999. Basin-scale surface water and energy budgets for the Mississippi from the ECMWF reanalysis. J. Geophys. Res. Atmos. 104 (D16), 19293–19306.

Bowen, I.S., 1926. The ratio of heat losses by conduction and by evaporation from any water surface. Phys. Rev. 27 (6), 779.

Burba, G.G., Verma, S.B., Kim, J., 1999. Surface energy fluxes of *Phragmites australis* in a prairie wetland. Agric. For. Meteorol. 94 (1), 31–51.

Capon, S.J., Chambers, L.E., Mac, Nally R., Naiman, R.J., Davies, P., Marshall, N., Pittock, J., Reid, M., Capon, T., Douglas, M., Catford, J., Baldwin, D.S., Stewardson, M., Roberts, J., Parsons, M., Williams, S.E., 2013. Riparian ecosystems in the 21st century: hotspots for climate change adaptation? Ecosystems 16 (3), 359–381.

Catford, J.A., Naiman, R.J., Chambers, L.E., Roberts, J., Douglas, M., Davies, P., 2013. Predicting novel riparian ecosystems in a changing climate. Ecosystems 16 (3), 382–400.

Cavanaugh, M.L., Kurc, S.A., Scott, R.L., 2011. Evapotranspiration partitioning in semiarid shrubland ecosystems: a two-site evaluation of soil moisture control on transpiration. Ecohydrology 4 (5), 671–681.

Chen, G.S., Chen, X.Q., Gou, X.J., 2008. Protection and Restoration of Eco-environment in Qinghai Lake Watershed. Qinghai People's Publishing House, Xining (In Chinese).

Cleverly, J.R., Dahm, C.N., Thibault, J.R., Mcdonnell, D.E., Allred Coonrod, J.E., 2006. Riparian ecohydrology: regulation of water flux from the ground to the atmosphere in the Middle Rio Grande, New Mexico. Hydrol. Process. 20 (15), 3207–3225.

Daamen, C.C., Dugas, W.A., Prendergast, P.T., Judd, M.J., Mcnaughton, K.G., 1999. Energy flux measurements in a sheltered lemon orchard. Agric. For. Meteorol. 93 (3), 171–183.

Dahm, C.N., Cleverly, J.R., Allred Coonrod, J.E., Thibault, J.R., Mcdonnell, D.E., Gilroy, D.J., 2002. Evapotranspiration at the land/water interface in a semi-arid drainage basin. Freshw. Biol. 47 (4), 831–843.

Dawson, T.E., 1996. Determining water use by trees and forests from isotopic, energy balance and transpiration analyses: the roles of tree size and hydraulic lift. Tree Physiol. 16 (1–2), 263–272.

De Vries, D., 1963. Thermal properties of soils. In: Van Wijk, W.R. (Ed.), Physics of the Plant Environment. North Holland, Amsterdam, pp. 210–235.

Domingo, F., Villagarcía, L., Brenner, A.J., Puigdefábregas, J., 1999. Evapotranspiration model for semi-arid shrub-lands tested against data from SE Spain. Agric. For. Meteorol. 95 (2), 67–84.

Drexler, J.Z., Snyder, R.L., Spano, D., Paw, U.K.T., 2004. A review of models and micrometeorological methods used to estimate wetland evapotranspiration. Hydrol. Process. 18 (11), 2071–2101.

Eugster, W., Rouse, W.R., Pielke Sr., R.A., Mcfadden, J.P., Baldocchi, D.D., Kittel, T.G.F., Chapin, F.S., Liston, G.E., Vidale, P.L., Vaganov, E., Chambers, S., 2000. Land–atmosphere energy exchange in Arctic tundra and boreal forest: available data and feedbacks to climate. Glob. Chang. Biol. 6 (S1), 84–115.

Feldhake, C.M., Boyer, D.G., 1986. Effect of soil temperature on evapotranspiration by C3 and C4 grasses. Agric. For. Meteorol. 37 (4), 309–318.

Frank, A.B., 2003. Evapotranspiration from Northern Semiarid Grasslands. Agron. J. 95 (6), 1504–1509.

Goodrich, D.C., Scott, R., Qi, J., Goff, B., Unkrich, C.L., Moran, M.S., Williams, D., Schaeffer, S., Snyder, K., Macnish, R., Maddock, T., Pool, D., Chehbouni, A., Cooper, D.I., Eichinger, W.E., Shuttleworth, W.J., Kerr, Y., Marsett, R., Ni, W., 2000. Seasonal estimates of riparian evapotranspiration using remote and in situ measurements. Agric. For. Meteorol. 105 (1–3), 281–309.

Gregory, S.V., Swanson, F.J., Mckee, W.A., Cummins, K.W., 1991. An ecosystem perspective of riparian zones. Bioscience 41 (8), 540–551.

Gu, S., Tang, Y., Cui, X., Kato, T., Du, M., Li, Y., Zhao, X., 2005. Energy exchange between the atmosphere and a meadow ecosystem on the Qinghai–Tibetan Plateau. Agric. For. Meteorol. 129 (3–4), 175–185.

Gu, S., Tang, Y., Cui, X., Du, M., Zhao, L., Li, Y., Xu, S., Zhou, H., Kato, T., Qi, P., Zhao, X., 2008. Characterizing evapotranspiration over a meadow ecosystem on the Qinghai–Tibetan Plateau. J. Geophys. Res.-Atmos. 113 (D08118D8).

Heilman, J.L., Brittin, C.L., Neale, C.M.U., 1989. Fetch requirements for Bowen ratio measurements of latent and sensible heat fluxes. Agric. For. Meteorol. 44 (3–4), 261–273.

Hu, Z., Yu, G., Zhou, Y., Sun, X., Li, Y., Shi, P., Wang, Y., Song, X., Zheng, Z., Zhang, L., Li, S., 2009. Partitioning of evapotranspiration and its controls in four grassland ecosystems: application of a two-source model. Agric. For. Meteorol. 149 (9), 1410–1420.

Johnson, R.K., Hering, D., Furse, M.T., Verdonschot, P., 2006. Indicators of ecological change: comparison of the early response of four organism groups to stress gradients. Hydrobiologia 566, 139–152.

Kang, S., Xu, Y., You, Q., Fl, U., Gel, W., Pepin, N., Yao, T., 2010. Review of climate and cryospheric change in the Tibetan Plateau. Environ. Res. Lett. 5 (1), 15101.

Kar, G., Kumar, A., 2007. Surface energy fluxes and crop water stress index in groundnut under irrigated ecosystem. Agric. For. Meteorol. 146 (1–2), 94–106.

Klein, J.A., Harte, J., Zhao, X., 2004. Experimental warming causes large and rapid species loss, dampened by simulated grazing, on the Tibetan Plateau. Ecol. Lett. 7 (12), 1170–1179.

Lenters, J.D., Cutrell, G.J., Istanbulluoglu, E., Scott, D.T., Herrman, K.S., Irmak, A., Eisenhauer, D.E., 2011. Seasonal energy and water balance of a *Phragmites australis*-dominated wetland in the republican river basin of south-central Nebraska (USA). J. Hydrol. 408 (1–2), 19–34.

Li, S.G., Asanuma, J., Kotani, A., Davaa, G., Oyunbaatar, D., 2007a. Evapotranspiration from a Mongolian steppe under grazing and its environmental constraints. J. Hydrol. 333 (1), 133–143.

Li, X., Xu, H., Sun, Y., Zhang, D., Yang, Z., 2007b. Lake-Level change and water balance analysis at Lake Qinghai, west China during recent decades. Water Resour. Manag. 21 (9), 1505–1516.

Li, S., Lü, S., Ao, Y., Shang, L., 2009a. Annual variations in the surface radiation budget and soil water and heat content in the Upper Yellow River area. Environ. Geol. 57 (2), 389–395.

Li, X.Y., Ma, Y., Xu, H.Y., Wang, J.H., Zhang, D.S., 2009b. Impact of land use and land cover change on environmental degradation in Lake Qinghai watershed, northeast Qinghai–Tibet Plateau. Land Degrad. Dev. 20 (1), 69–83.

Li, J., Jiang, S., Wang, B., Jiang, W.W., Tang, Y.H., Du, M.Y., Gu, S., 2013. Evapotranspiration and its energy exchange in alpine meadow ecosystem on the Qinghai–Tibetan Plateau. J. Integr. Agric. 12 (8), 1396–1401.

Liu, S., Li, S.G., Yu, G.R., Sun, X.M., Zhang, L.M., Hu, Z.M., Li, Y.N., Zhang, X.Z., 2009. Surface energy exchanges above two grassland ecosystems on the Qinghai–Tibetan Plateau. Biogeosci. Discuss. 6 (5), 9161–9192.

Liu, S., Li, S., Yu, G., Zhang, L., Sugita, M., Li, Y., Zhang, X., Wang, Y., 2010. Surface energy exchanges in grassland ecosystems along a precipitation gradient. Acta Ecol. Sin. 30 (3), 557–567 (In Chinese with English abstract).

Ma, W., Ma, Y., 2006. The annual variations on land surface energy in the northern Tibetan Plateau. Environ. Geol. 50 (5), 645–650.

Ma, Y., Su, Z., Koike, T., Yao, T., Ishikawa, H., Ueno, K.I., Menenti, M., 2003. On measuring and remote sensing surface energy partitioning over the Tibetan Plateau—from GAME/Tibet to CAMP/Tibet. Phys. Chem. Earth 28 (1–3), 63–74.

Malek, E., Bingham, G.E., 1993. Comparison of the Bowen ratio-energy balance and the water balance methods for the measurement of evapotranspiration. J. Hydrol. 146, 209–220.

Mander, Ü., Kuusemets, V., Lõhmus, K., Mauring, T., 1997. Efficiency and dimensioning of riparian buffer zones in agricultural catchments. Ecol. Eng. 8 (4), 299–324.

Meehan, W.R., Swanson, F.J., Sedell, J.R., 1977. Influences of riparian vegetation on aquatic ecosystems with particular reference to salmonid fishes and their food supply. In: Johnson, R.R., Jones, D.A. (Eds.), Importance, Preservation and Management of Riparian Habitat: A Symposium. USDA Forest Service General Technical Report RM-43. Tuscon, Arizona, pp. 137–145.

Nilsson, C., Jansson, R., Kuglerova, L., Lind, L., Strom, L., 2013. Boreal riparian vegetation under climate change. Ecosystems 16 (3), 401–410.

Ohmura, A., 1982. Objective criteria for rejecting data for Bowen ratio flux calculations. J. Appl. Meteorol. 21 (4), 595–598.

Peacock, C.E., Hess, T.M., 2004. Estimating evapotranspiration from a reed bed using the Bowen ratio energy balance method. Hydrol. Process. 18 (2), 247–260.

Perez, P.J., Castellvi, F., Ibañez, M., Rosell, J.I., 1999. Assessment of reliability of Bowen ratio method for partitioning fluxes. Agric. For. Meteorol. 97 (3), 141–150.

Pielke Sr., R.A., Avissar, R., Raupach, M., Dolman, A.J., Zeng, X., Denning, A.S., 1998. Interactions between the atmosphere and terrestrial ecosystems: influence on weather and climate. Glob. Chang. Biol. 4 (5), 461–475.

Prueger, J.H., Hatfield, J.L., Aase, J.K., Pikul, J.L., 1997. Bowen-ratio comparisons with lysimeter evapotranspiration. Agron. J. 89 (5), 730–736.

Qiu, G.Y., Xie, F., Feng, Y.C., Tian, F., 2011. Experimental studies on the effects of the "conversion of cropland to grassland program" on the water budget and evapotranspiration in a semi-arid steppe in Inner Mongolia, China. J. Hydrol. 411 (1–2), 120–129.
Rohli, R.V., Hsu, S.A., Lofgren, B.M., Binkley, M.R., 2004. Bowen ratio estimates over Lake Erie. J. Great Lakes Res. 30 (2), 241–251.
Savage, M.J., 2010. Field evaluation of polymer capacitive humidity sensors for Bowen ratio energy balance flux measurements. Sensors 10 (8), 7748–7771.
Savage, M.J., Everson, C.S., Metelerkamp, B.R., 2009. Bowen ratio evaporation measurement in a remote montane grassland: data integrity and fluxes. J. Hydrol. 376 (1–2), 249–260.
Scott, R.L., Cable, W.L., Huxman, T.E., Nagler, P.L., Hernandez, M., Goodrich, D.C., 2008. Multiyear riparian evapotranspiration and groundwater use for a semiarid watershed. J. Arid Environ. 72 (7), 1232–1246.
Serrat-Capdevila, A., Scott, R.L., Shuttleworth, W.J., Valdes, J.B., 2011. Estimating evapotranspiration under warmer climates: insights from a semi-arid riparian system. J. Hydrol. 399 (1–2), 1–11.
Si, J.H., Feng, Q., Zhang, X.Y., Liu, W., Su, Y.H., Zhang, Y.W., 2005. Growing season evapotranspiration from *Tamarix ramosissima* stands under extreme and conditions in northwest China. Environ. Geol. 48 (7), 861–870.
Stannard, D., 1997. A theoretically based determination of Bowen-ratio fetch requirements. Bound.-Layer Meteorol. 83 (3), 375–406.
Stannard, D., Rosenberry, D., Winter, T., Parkhurst, R., 2004. Estimates of fetch-induced errors in Bowen-ratio energy-budget measurements of evapotranspiration from a prairie wetland, Cottonwood Lake Area, North Dakota, USA. Wetlands 24 (3), 498–513.
Staudinger, M., Rott, H., 1981. Evapotranspiration at two mountain sites during the vegetation period. Nord. Hydrol. 12 (4–5), 207–216.
Swanson, F.J., Gregory, S.V., Sedell, J.R., Campbell, A.G., 1982. Land–water interactions: the riparian zone. In: Edmonds, R.L. (Ed.), Analysis of Coniferous Forest Ecosystems in the Western United States. US/IBP Synthesis Series 14. Hutchinson Ross Publishing Co., Stroudsburg, PA, pp. 267–291.
Tanaka, K., Ishikawa, H., Hayashi, T., Tamagawa, I., Ma, Y., 2001. Surface energy budget at Amdo on the Tibetan Plateau using GAME/Tibet IOP98 data. J. Meteorol. Soc. Jpn. 79 (1B), 505–517.
Tanaka, K., Tamagawa, I., Ishikawa, H., Ma, Y., Hu, Z., 2003. Surface energy budget and closure of the eastern Tibetan Plateau during the GAME-Tibet IOP 1998. J. Hydrol. 283 (1–4), 169–183.
Tian, F.X., Zhao, C.Y., Feng, Z.D., 2011. Simulating evapotranspiration of Qinghai spruce (*Picea crassifolia*) forest in the Qilian Mountains, northwestern China. J. Arid Environ. 75 (7), 648–655.
Todd, R.W., Evett, S.R., Howell, T.A., 2000. The Bowen ratio-energy balance method for estimating latent heat flux of irrigated alfalfa evaluated in a semi-arid, advective environment. Agric. For. Meteorol. 103 (4), 335–348.
Wang, Z.Q., 2003. Estimation of Hydraulic Characteristic Properties of the Keerqin Sandy Land. Inner Mongolia Agricultural University, Huhhot (In Chinese with English abstract).
Wang, S.S., Zhu, Z.L., Sun, X.M., 1996. Characteristics of energy and mass exchanges in the wheat field of Lhasa, Xizang (Tibet). Sci. China Ser. D Earth Sci. 39 (4), 418–424.
Williams, D.G., Scott, R.L., Huxman, T.E., Goodrich, D.C., Lin, G., 2006. Sensitivity of riparian ecosystems in arid and semiarid environments to moisture pulses. Hydrol. Process. 20 (15), 3191–3205.
Wu, T., Zhao, L., Li, R., Wang, Q., Xie, C., Pang, Q., 2013. Recent ground surface warming and its effects on permafrost on the central Qinghai–Tibet Plateau. Int. J. Climatol. 33 (4), 920–930.
Xing, Z., Chow, L., Meng, F., Rees, H.W., Steve, L., Monteith, J., 2008. Validating evapotranspiraiton equations using Bowen ratio in New Brunswick, Maritime, Canada. Sensors 8 (1), 412–428.
Yang, Y., Chen, R., 2011. Research review on hydrology in the permafrost and seasonal frozen regions. Adv. Earth Sci. 26 (7), 711–723 (In Chinese with English abstract).
Yang, M., Yao, T., He, Y., 2002. The role of soil moisture—energy distribution and melting—freezing processes on seasonal shift in Tibetan Plateau. J. Mt. Sci. 20 (5), 553–558 (In Chinese with English abstract).
Yao, J., Zhao, L., Ding, Y., Gu, L., Jiao, K., Qiao, Y., Wang, Y., 2008. The surface energy budget and evapotranspiration in the Tanggula region on the Tibetan Plateau. Cold Reg. Sci. Technol. 52 (3), 326–340.
Yi, W., 2011. Evaluation of Carrying Capacity and Allocation of Water Resources in QingHai Lake Watershed. Beijing Normal University, Beijing (In Chinese with English abstract).
Yoshida, M., Ohta, T., Kotani, A., Maximov, T., 2010. Environmental factors controlling forest evapotranspiration and surface conductance on a multi-temporal scale in growing seasons of a Siberian larch forest. J. Hydrol. 395 (3–4), 180–189.
You, Q., Kang, S., Pepin, N., Flügel, W., Sanchez-Lorenzo, A., Yan, Y., Zhang, Y., 2010. Climate warming and associated changes in atmospheric circulation in the eastern and central Tibetan Plateau from a homogenized dataset. Glob. Planet. Chang. 72 (1–2), 11–24.
Zhang, Y., Li, B., Zheng, D., 2002. A discussion on the boundary and area of the Tibetan Plateau in China. Geogr. Res. 21 (1), 1–8 (In Chinese with English abstract).
Zhang, Y., Ohata, T., Kadota, T., 2003. Land-surface hydrological processes in the permafrost region of the eastern Tibetan Plateau. J. Hydrol. 283 (1–4), 41–56.
Zhang, X., Chen, D.Q., Yan, L., Liu, S.P., Duan, X.F., 2005. The problem and strategies to protect the Naked Carp of Qinghai Lake (*Gymnocypris przewalskii*). Freshw. Fish. 35 (4), 57–60 (In Chinese).
Zhang, B., Kang, S., Li, F., Zhang, L., 2008. Comparison of three evapotranspiration models to Bowen ratio-energy balance method for a vineyard in an arid desert region of northwest China. Agric. For. Meteorol. 148 (10), 1629–1640.
Zhang, G., Xie, H., Duan, S., Tian, M., Yi, D., 2011a. Water level variation of Lake Qinghai from satellite and in situ measurements under climate change. J. Appl. Remote. Sens. 5 (1), 53532.
Zhang, K., Kimball, J.S., Kim, Y., Mcdonald, K.C., 2011b. Changing freeze–thaw seasons in northern high latitudes and associated influences on evapotranspiration. Hydrol. Process. 25 (26), 4142–4151.
Zhao, G., Li, X., Wu, H., Zhang, S., Li, G., 2013. Study on plant water use in *Myricaria squamosa* with stable hydrogen isotope tracer in Qinghai Lake basin. Chin. J. Plant Ecol. 37 (12), 1091–1100 (In Chinese with English abstract).
Zhou, J., Wang, G., Li, X., Yang, Y., Pan, X., 2008. Energy-water balance of meadow ecosystem in cold frozen soil areas. J. Glaciol. Geocryol. 30 (3), 398–407 (In Chinese with English abstract).